Received: 19 September 2022 | Accepted: 10 October 2022

DOI: 10.1002/pamm.202200015

A novel anisotropic stress-driven model for bioengineered tissues accounting for remodeling and reorientation based on homeostatic surfaces

Hagen Holthusen[1,*], **Christiane Rothkranz**[1], **Lukas Lamm**[1], **Tim Brepols**[1], and **Stefanie Reese**[1]

[1] Institute of Applied Mechanics, RWTH Aachen University, Mies-van-der-Rohe-Str. 1, 52074 Aachen, Germany

A co-rotated formulation of the intermediate configuration is derived in a thermodynamically consistent manner. As a result of this formulation, algorithmic differentiation (AD) and the equations of the material model can be combined directly, i.e., the equations can be implemented into the AD tool and the corresponding derivatives can be calculated using AD. This is not possible when the equations are given in terms of the intermediate configuration, since the multiplicative decomposition suffers from an inherent rotational non-uniqueness. Moreover, a novel stress-driven kinematic growth model is presented that takes homeostasis and fiber reorientation into account and is based on the co-rotated formulation. A numerical example reveals the promising potential of both the co-rotated formulation and the stress-driven growth model.

1 Introduction

In the last decades, the modeling of finite inelastic material behavior has become more and more advanced. In this regard, the multiplicative decomposition of the deformation gradient has emerged as an extremely powerful continuum mechanical approach. This approach is used in various disciplines reaching from elasto-plasticity coupled with damage (e.g. [1]) to the modeling of soft tissues' growth and remodeling (e.g. [2]). To tackle the challenging and error-prone numerical implementation of such models, AD has proven to be a handy tool, which unfortunately cannot be easily combined with models based on the multiplicative decomposition. The reason lies in the involved rotational non-uniqueness of the decomposition.

One of the currently most challenging tasks of material modeling is the simulation of soft biological tissues. Soft tissues are known to seek for a certain state of homeostasis (see e.g. [3]). In order to achieve this state, which is characterized by a preferred stress state to be reached throughout the tissue, the tissue growths and remodels itself until this state is reached. In the literature, different approaches exist to describe these phenomena, for instance, constraint mixture approaches. In this regard, [4] recently published an approach based on so-called homeostatic surfaces. These surfaces prescribe the preferred state in the principal stress space, such that growth and remodeling is considered in a smeared and phenomenological sense until the current stress state coincides with the surface. Additionally, soft tissue are able to remodel collagen fibers – often referred to as reorientation – in order to increase their mechanical resistance to changing loading conditions.

Within this contribution, a novel co-rotated formulation of the intermediate configuration is presented at first. This configuration is unique, but shares the same physical interpretation with the intermediate one. Hence, contrary to equations stated with respect to the intermediate configuration, material model equations in the co-rotated configuration can be directly implemented into an AD tool. This enables an efficient and easy numerical implementation of a wide class of materials.

Second, a new stress-driven growth and remodeling model is discussed. Its theoretical backbone is the co-rotated intermediate configuration. Furthermore, the approach of homeostatic surfaces is followed and the preferred stress state is prescribed in terms of the overall Cauchy stress in the principal stress state. Here, the hypothesis of tensile homeostasis is followed. Moreover, reorientation of collagen fibers is taken into account such that these fibers align with the principal tensile direction.

Section 2 presents the co-rotated formulation, and further, discusses the influence of structural tensors. Subsequently, in Section 3, a novel stress-driven growth and remodeling model is developed. Further, the evolution equations of the different inelastic phenomena are discussed. Finally, the models is investigated in a three-dimensional setting in Section 4.

2 Co-rotational formulation of the intermediate configuration

Within this contribution, the well-established multiplicative decomposition of the deformation gradient $\boldsymbol{F}$ into its elastic $\boldsymbol{F}_e$ and growth-related part $\boldsymbol{F}_g$ is employed (see [5]). For the time being, the Helmholtz free energy ψ is assumed to be a *scalar-valued isotropic function* of the elastic Cauchy-Green tensor $\boldsymbol{C}_e \coloneqq \boldsymbol{F}_e^T\boldsymbol{F}_e = \boldsymbol{F}_g^{-T}\boldsymbol{C}\boldsymbol{F}_g^{-1}$ with $\boldsymbol{C} \coloneqq \boldsymbol{F}^T\boldsymbol{F}$ and some structural tensor $\breve{\boldsymbol{M}} \coloneqq \boldsymbol{F}_g\boldsymbol{M}\boldsymbol{F}_g^T/\mathrm{tr}(\boldsymbol{C}_g\boldsymbol{M})$ with $\boldsymbol{C}_g \coloneqq \boldsymbol{F}_g^T\boldsymbol{F}_g$ and $\boldsymbol{M}$ being a (symmetric) structural tensor in the reference configuration. Its purpose is to take into account the orientation of the fibers. The mapping of $\boldsymbol{M}$ from the reference to the intermediate configuration is chosen in line with [6].

* Corresponding author: e-mail hagen.holthusen@ifam.rwth-aachen.de, phone +49 241 80 25016, fax +49 241 80 22001

Unfortunately, the multiplicative decomposition of $\boldsymbol{F}$ suffers from an inherent non-uniqueness, i.e.

$$\boldsymbol{F} = \boldsymbol{F}_e\boldsymbol{F}_g = \boldsymbol{F}_e\boldsymbol{Q}^T\boldsymbol{Q}\boldsymbol{F}_g =: \boldsymbol{F}_e^*\boldsymbol{F}_g^*, \quad \boldsymbol{Q} \in \mathrm{SO}(3) \tag{1}$$

is an equivalent decomposition as well. Due to this non-uniqueness, neither $\boldsymbol{C}_e$ nor $\breve{\boldsymbol{M}}$ can be determined, and thus, also $\psi = \bar{\psi}(\boldsymbol{C}_e, \breve{\boldsymbol{M}})$ cannot be calculated[1]. Hence, it is not straightforward to implement the material model's equations derived with respect to the intermediate configuration directly into an AD tool. To solve this, additional pull-back operations of all constitutively dependent variables are necessary (cf. [7]). However, besides the additional effort, the thermodynamic driving forces might lose their physical meaning as well as their symmetry properties.

Therefore, the aim is to present a co-rotated formulation of the intermediate configuration in the following. Contrary to the latter, this co-rotated configuration is uniquely defined, but at the same time has the same physical interpretation as the intermediate configuration. Further, all symmetry properties are preserved. To begin with, using the polar decomposition $\boldsymbol{F}_g = \boldsymbol{R}_g\boldsymbol{U}_g$ with $\boldsymbol{R}_g \in \mathrm{SO}(3)$, it can be seen that only the rotation tensor $\boldsymbol{R}_g$ is affected by the non-uniqueness, while the growth-related stretch tensor $\boldsymbol{U}_g$ is uniquely defined. Thus, the co-rotated quantities $\bar{\boldsymbol{C}}_e := \boldsymbol{R}_g^T\boldsymbol{C}_e\boldsymbol{R}_g = \boldsymbol{U}_g^{-1}\boldsymbol{C}\boldsymbol{U}_g^{-1}$ and $\bar{\boldsymbol{M}} := \boldsymbol{R}_g^T\breve{\boldsymbol{M}}\boldsymbol{R}_g = \boldsymbol{U}_g\boldsymbol{M}\boldsymbol{U}_g/\mathrm{tr}(\boldsymbol{C}_g\boldsymbol{M})$ are introduced. Since these quantities are *similar* with their intermediate counterparts, the same Helmholtz free energy can be used, i.e. $\psi = \bar{\psi}(\boldsymbol{C}_e, \breve{\boldsymbol{M}}) = \bar{\psi}(\bar{\boldsymbol{C}}_e, \bar{\boldsymbol{M}})$. Inserting this Helmholtz free energy into the Clausius-Planck inequality $-\dot{\psi} + 1/2\,\boldsymbol{S} : \dot{\boldsymbol{C}} \geq 0$, the following state law for the second Piola-Kirchhoff stress $\boldsymbol{S}$ as well as the thermodynamic driving forces are obtained

$$\boldsymbol{S} = 2\,\boldsymbol{U}_g^{-1}\frac{\partial\psi}{\partial\bar{\boldsymbol{C}}_e}\boldsymbol{U}_g^{-1}, \quad \bar{\boldsymbol{\Sigma}} := 2\,\bar{\boldsymbol{C}}_e\frac{\partial\psi}{\partial\bar{\boldsymbol{C}}_e}, \quad \bar{\boldsymbol{\Pi}} := 2\frac{\partial\psi}{\partial\bar{\boldsymbol{M}}}\bar{\boldsymbol{M}} - 2\frac{\partial\psi}{\partial\bar{\boldsymbol{M}}} : (\bar{\boldsymbol{M}} \otimes \bar{\boldsymbol{M}}), \quad \bar{\boldsymbol{\Gamma}} := \bar{\boldsymbol{\Sigma}} - \bar{\boldsymbol{\Pi}} \tag{2}$$

where the relative stress $\bar{\boldsymbol{\Gamma}}$ is conjugated to $\bar{\boldsymbol{D}}_g := \mathrm{sym}(\dot{\boldsymbol{U}}_g\boldsymbol{U}_g^{-1})$. Furthermore, the conjugated driving forces in the latter equation can be considered the co-rotated quantities of their intermediate counterparts, e.g. $\bar{\boldsymbol{\Sigma}} = \boldsymbol{R}_g^T(2\,\boldsymbol{C}_e(\partial\psi/\partial\boldsymbol{C}_e))\boldsymbol{R}_g$. It should be mentioned that the driving force associated with $\dot{\boldsymbol{M}}$ is unique as well and can also be computed using AD. However, since this driving force is not needed in the model presented hereafter, it is omitted at this point.

Since all quantities in Equation (2) are uniquely defined as well, all of them can be implemented into an AD tool without further pull-back operations. Moreover, all derivatives of the Helmholtz free energy can be calculated using AD, which is considered a major advantage, since these might be challenging when computed 'by hand'. With this framework of a co-rotated intermediate configuration at hand, the following Section 3 considers a novel stress-driven kinematic growth model, which is based on the proposed co-rotated framework, and thus, fully implemented using AD.

Note on numerical implementation. Since an AD tool is utilized for the numerical implementation, only some scalar-valued inelastic potentials as well as the Helmholtz free energy need to be prescribed. All derivatives appeared so far are uniquely defined, and thus, can be calculated by AD. The same holds for the derivatives of the material model proposed hereafter. For the time discretized evolution equation of $\bar{\boldsymbol{D}}_g$, an exponential integrator scheme similar to [7] is utilized. Thus, an efficient and flexible implementation of the overall model is enabled.

3 Stress-driven growth model

This sections deals with a novel stress-driven growth and remodeling model for soft tissues as well as the reorientation of collagen fibers in a stress-driven manner. In this regards, soft tissues are considered in a smeared sense. Hence, for modeling growth and remodeling, two parallel decomposition of the deformation gradient into 'matrix' (m) and 'fibers' (f) parts are utilized, i.e.

$$\boldsymbol{F} = \boldsymbol{F}_{e_m}\boldsymbol{F}_{g_m} = \boldsymbol{F}_{e_f}\boldsymbol{F}_{g_f}. \tag{3}$$

Direction-independent constituents such as elastin are summarized within the first decomposition, while the second decomposition accounts for direction-dependent constituents like collagen. The Helmholtz free energy is assumed to be additively decomposed, i.e. $\psi = \psi_m(\bar{\boldsymbol{C}}_{e_m}) + \psi_f(\bar{\boldsymbol{C}}_{e_f}, \bar{\boldsymbol{M}})$ where the contribution of the 'matrix' is given by ψ_m and ψ_f accounts for the 'fibers' contribution. Moreover, the structural tensor in the reference configuration is defined by $\boldsymbol{M} = \boldsymbol{n} \otimes \boldsymbol{n}$ with $\boldsymbol{n}$ being the structural vector in the reference configuration, which is parallel to the (major) collagen direction. Similar to the procedure described in the previous section, and as a result of the parallel decomposition in Equation (3), the driving forces and the second Piola-Kirchhoff stress read

$$\boldsymbol{S} = 2\,\boldsymbol{U}_{g_m}^{-1}\frac{\partial\psi}{\partial\bar{\boldsymbol{C}}_{e_m}}\boldsymbol{U}_{g_m}^{-1} + 2\,\boldsymbol{U}_{g_f}^{-1}\frac{\partial\psi}{\partial\bar{\boldsymbol{C}}_{e_f}}\boldsymbol{U}_{g_f}^{-1}, \quad \bar{\boldsymbol{\Gamma}}_m := 2\,\bar{\boldsymbol{C}}_{e_m}\frac{\partial\psi}{\partial\bar{\boldsymbol{C}}_{e_m}}, \quad \bar{\boldsymbol{\Gamma}}_f := 2\,\bar{\boldsymbol{C}}_{e_f}\frac{\partial\psi}{\partial\bar{\boldsymbol{C}}_{e_f}} - \bar{\boldsymbol{\Pi}} \tag{4}$$

with $\bar{\boldsymbol{C}}_{e_m} := \boldsymbol{U}_{g_m}^{-1}\boldsymbol{C}\boldsymbol{U}_{g_m}^{-1}$ and $\bar{\boldsymbol{C}}_{e_f} := \boldsymbol{U}_{g_f}^{-1}\boldsymbol{C}\boldsymbol{U}_{g_f}^{-1}$. The stretch tensors $\boldsymbol{U}_{g_m}$ and $\boldsymbol{U}_{g_f}$ result from the polar decompositions of $\boldsymbol{F}_{g_m}$ and $\boldsymbol{F}_{g_f}$, respectively. Moreover, it is important to note that both $\bar{\boldsymbol{\Gamma}}_m$ and $\bar{\boldsymbol{\Gamma}}_f$ are symmetric (cf. [8]). It remains to choose suitable evolution equations for growth and remodeling as well as fiber reorientation, which will be presented in the following.

[1] Since ψ is an *isotropic function*, changing the arguments $\psi = \psi^{\#}(\boldsymbol{C}, \boldsymbol{C}_g, \boldsymbol{M})$ allows to determine ψ depending on referential quantities (cf. [7]).

3.1 Evolution equations

Soft biological tissues are known to prefer a state of homeostasis, i.e. a homeostatic stress is tried to reach throughout the whole tissue. Within this contribution, the approach suggested in [4] for modeling growth and remodeling is followed. A so-called 'homeostatic surface' in the principal stress space similar to plasticity is introduced, which describes the preferred or homeostatic stress. Due to growth and remodeling, the tissues seeks to achieve this preferred state. The direction of growth may be described in an associative way by taking the derivative of the homeostatic surface with respect to the thermodynamic driving forces.

Besides growth and remodeling, collagen fibers are produced and absorbed by cells in order to optimally carry mechanical loading. In a smeared sense, this can be described by a reorientation of the structural vector associated with the direction of collagen fibers. Here, it is assumed that an optimal state is reached when the structural vector is collinear with the eigenvector associated with the principal eigenvalue of Cauchy's stress tensor $\boldsymbol{\sigma} = 1/J\,\boldsymbol{\tau} = 1/J\,\boldsymbol{F}\boldsymbol{S}\boldsymbol{F}^T$. In the latter equation, J is the determinate of $\boldsymbol{F}$ and $\boldsymbol{\tau}$ the Kirchhoff stress tensor.

Growth and remodeling. The homeostatic surface proposed herein is assumed to be a *scalar-valued isotropic function* of the overall Cauchy stress $\boldsymbol{\sigma}$. To account for the hypothesis of tensile homeostasis, i.e. a tensile stress state is preferred (cf. [3]), the following smoothed Rankine-like surface is introduced

$$\Phi = \operatorname{tr}(\boldsymbol{\sigma}) + \sqrt{\operatorname{tr}(\boldsymbol{\sigma}^2) + \beta} - 2\,\sigma_{hom} \tag{5}$$

where σ_{hom} is the homeostatic stress and β is a stress-like parameter for shifting the surface in the principal stress space. Further, having in mind that $\boldsymbol{\tau} = 2\left(\boldsymbol{F}_{e_m}(\partial\psi/\partial\boldsymbol{C}_{e_m})\boldsymbol{F}_{e_m}^T + \boldsymbol{F}_{e_f}(\partial\psi/\partial\boldsymbol{C}_{e_f})\boldsymbol{F}_{e_f}^T\right)$ with $\boldsymbol{C}_{e_m} \coloneqq \boldsymbol{F}_{e_m}^T\boldsymbol{F}_{e_m}$ and $\boldsymbol{C}_{e_f} \coloneqq \boldsymbol{F}_{e_f}^T\boldsymbol{F}_{e_f}$, the following relation is important to note

$$\boldsymbol{\tau} = \boldsymbol{F}^{-T}\left(\boldsymbol{U}_{g_m}\bar{\boldsymbol{\Gamma}}_m\boldsymbol{U}_{g_m}^{-1} + \boldsymbol{U}_{g_f}\left(\bar{\boldsymbol{\Gamma}}_f + \bar{\boldsymbol{\Pi}}\right)\boldsymbol{U}_{g_f}^{-1}\right)\boldsymbol{F}^T. \tag{6}$$

The term in brackets is generally non-symmetric, but shares the same eigenvalues with $\boldsymbol{\tau}$. Hence, the following evolution equations for the co-rotated symmetric parts of the inelastic velocity gradients $\bar{\boldsymbol{D}}_{g_m} \coloneqq \operatorname{sym}\left(\dot{\boldsymbol{U}}_{g_m}\boldsymbol{U}_{g_m}^{-1}\right)$ and $\bar{\boldsymbol{D}}_{g_f} \coloneqq \operatorname{sym}\left(\dot{\boldsymbol{U}}_{g_f}\boldsymbol{U}_{g_f}^{-1}\right)$ are introduced

$$\bar{\boldsymbol{D}}_{g_m} = \dot{\gamma}\frac{\partial\Phi}{\partial\bar{\boldsymbol{\Gamma}}_m}\Bigg/\,\|\frac{\partial\Phi}{\partial\bar{\boldsymbol{\Gamma}}_m}\|, \quad \bar{\boldsymbol{D}}_{g_f} = \dot{\gamma}\frac{\partial\Phi}{\partial\bar{\boldsymbol{\Gamma}}_f}\Bigg/\,\|\frac{\partial\Phi}{\partial\bar{\boldsymbol{\Gamma}}_f}\|. \tag{7}$$

In the latter equations, $\dot{\gamma}$ is a kind of growth multiplier that describes the rate of growth and remodeling. The multiplier is determined by a Perzyna-type law (see [9]): $\dot{\gamma} = 1/\eta\,(\Phi/2\,\sigma_{hom})$. Here, η is the growth and remodeling time.

Reorientation. As mentioned above, fiber reorientation is considered in a stress-driven manner. Therefore, a physically reasonable evolution equation of the structural vector is stated in the current configuration. More precisely, an optimal state is reached if the structural vector in the current configuration is parallel to Cauchy's principal eigenvector. Unfortunately, in this case objective rates must be taken into account. To avoid this issue, the polar decomposition $\boldsymbol{F} = \boldsymbol{R}\boldsymbol{U}$ with $\boldsymbol{R} \in \mathrm{SO}(3)$ is employed. Based on this decomposition, the so-called co-rotated Cauchy stress $\boldsymbol{R}^T\boldsymbol{\sigma}\boldsymbol{R}$ as well as the (normalized) stretched structural vector $\boldsymbol{n}' \coloneqq (1/\sqrt{\boldsymbol{n}\cdot\boldsymbol{C}\cdot\boldsymbol{n}})\,\boldsymbol{U}\boldsymbol{n}$ are introduced. Noteworthy, it can be shown that an optimal state is also reached if the principal eigenvector of the co-rotated Cauchy stress and $\boldsymbol{n}'$ are collinear. It should be noted that it is assumed that the collagen fibers always align with the principal tensile direction. In the case of a fully compressive state, no reorientation takes place.

The evolution equation is chosen in line with [10]

$$\dot{\boldsymbol{n}}' = \frac{\pi}{2\tau}\,(\boldsymbol{n}' \times \boldsymbol{n}_t) \times \boldsymbol{n}' \tag{8}$$

with the reorientation time τ. Note that the latter equation can be reformulated in terms of a skew-symmetric tensor contracted with $\boldsymbol{n}'$. Hence, if an exponential integrator scheme is utilized for the time discretized evolution equation, this can be solved in closed-form using Rodrigues' formula. Further, $\boldsymbol{n}_t$ is the principal eigenvector of Cauchy's stress tensor.

3.2 Specific choices for energy terms

For studying the material model's response, the following Helmholtz free energy terms are chosen. For the 'matrix' part, a compressible Neo-Hookean energy is used

$$\psi_m = \frac{\mu_m}{2}\left(\operatorname{tr}\left(\bar{\boldsymbol{C}}_{e_m}\right) - 3 - \ln\left(\det\left(\bar{\boldsymbol{C}}_{e_m}\right)\right)\right) + \frac{\Lambda_m}{4}\left(\det\left(\bar{\boldsymbol{C}}_{e_m}\right) - 1 - \ln\left(\det\left(\bar{\boldsymbol{C}}_{e_m}\right)\right)\right) \tag{9}$$

while the energy for the 'fibers' part is in line with [11]

$$\psi_f = \frac{K_1}{2\,K_2}\,\left(\exp\left(K_2\langle \mathrm{tr}\left(\bar{\boldsymbol{C}}_{e_f}\bar{\boldsymbol{M}}\right)-1\rangle^2\right)-1\right). \tag{10}$$

In the latter, the Macaulay brackets are used, since collagen fibers are assumed to be not able to carry compressive loadings. The material parameters are μ_m, Λ_m, K_1 and K_2.

4 Numerical example

In this contribution, the boundary value problem considered is chosen in accordance with the example presented e.g. in [12]. The corresponding geometry as well as the loading applied are illustrated in Figure 1. Here, the radial displacement loading is described by $u_r(z) = 0.3\,\sin(\pi/4\;z)$ [mm] such that the maximum displacement is 0.3 [mm]. Both the top and bottom surfaces are considered clamped.

The material parameters are either taken from the literature [12] or arbitrarily chosen: $\Lambda_m = 4.285$ [MPa], $\mu_m = 1.071$ [MPa], $K_1 = 2.0$ [MPa], $K_2 = 1.0$ [-], $\sigma_{hom} = 1.0$ [MPa], $\eta = 10.0$ [h], $\beta = 0.1$ [MPa], $\tau = 10.0$ [h]. The initial collagen fiber directions are randomly chosen per element. Furthermore, a reduced integrated finite element formulation with a single Gaussian point per element [13] is utilized for discretization to avoid locking effects.

The loading is increased in a monotonic way within the first hour, i.e. the load is linearly increased until the maximum displacement of 0.3 [mm] is reached at $t = 1$ [h]. Subsequently, the loading is hold constant until the end of the simulation. Furthermore, the force-time curve obtained throughout the simulation up to $t = 40$ [h] is shown in Figure 2. As can be seen, due to growth and remodeling as well as fiber reorientation, a tensile state is observed at the beginning, while a compressive state is reached in the longitudinal direction at the end. Moreover, since the slope is decreasing at the end, it can concluded that a state of homeostasis is reached. In order to give a better understanding of the processes, Figure 3 provides the contour plots of the Cauchy stress in longitudinal direction σ_{zz} and the value of the growth multiplier $\dot{\gamma}$. Noteworthy, the multiplier is always non-zero if the current stress state does not lie on the homeostatic surface, i.e. homeostasis is not reached.

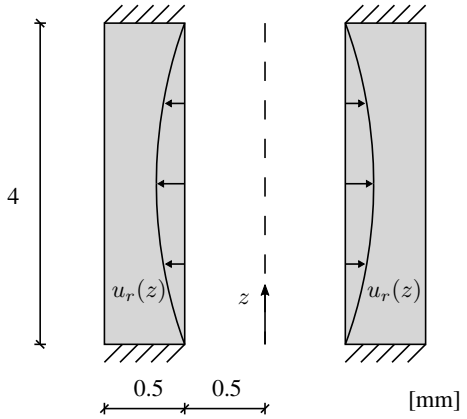

Fig. 1: Geometry and boundary value problem. The geometry and loading are axisymmetric with z being the axis of symmetry. The displacement in radial direction is sine-shaped. For meshing, 4 elements in thickness direction, 16 elements over the height and 32 elements in circumferential direction are used.

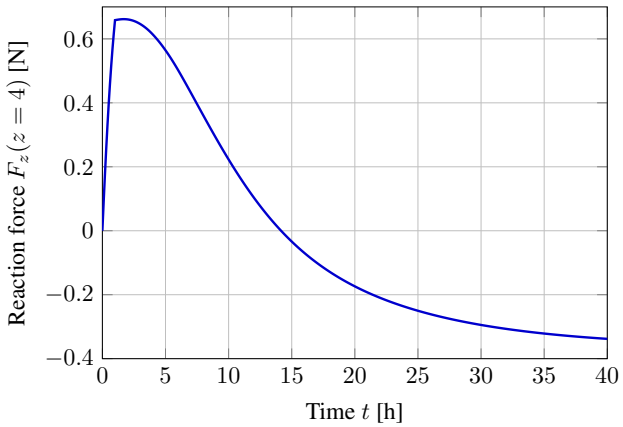

Fig. 2: Force-time curve at the top surface ($z = 4$ [mm]). Within the first hour, the sine-shaped loading is linearly increased and then hold constant throughout the rest of the simulation.

At the beginning ($t = 1$ [h]), the fibers are randomly orientated. Further, the stress state is far from lying on the chosen homeostatic, since the rate of $\dot{\gamma}$ is relatively high and mainly depends on the over- and under-stress, respectively. With time, the collagen fibers orient themselves towards the principal tensile direction of stress, which is the circumferential one. At the end of the simulation, nearly all fibers are aligned with this particular direction.

Since the rate of growth and remodeling is highest in the middle of the specimen, growth and remodeling are most pronounced in this region. However, at the end of the simulation homeostasis is reached throughout the whole specimen. Similarly, stress is initially quite heterogeneous in the longitudinal direction, but becomes more homogeneous as homeostasis is reached and collagen fibers are aligned in circumferential direction.

In summary, it can be concluded that the model is able to provide plausible results in terms of homeostasis and fiber reorientation for complex loading scenarios.

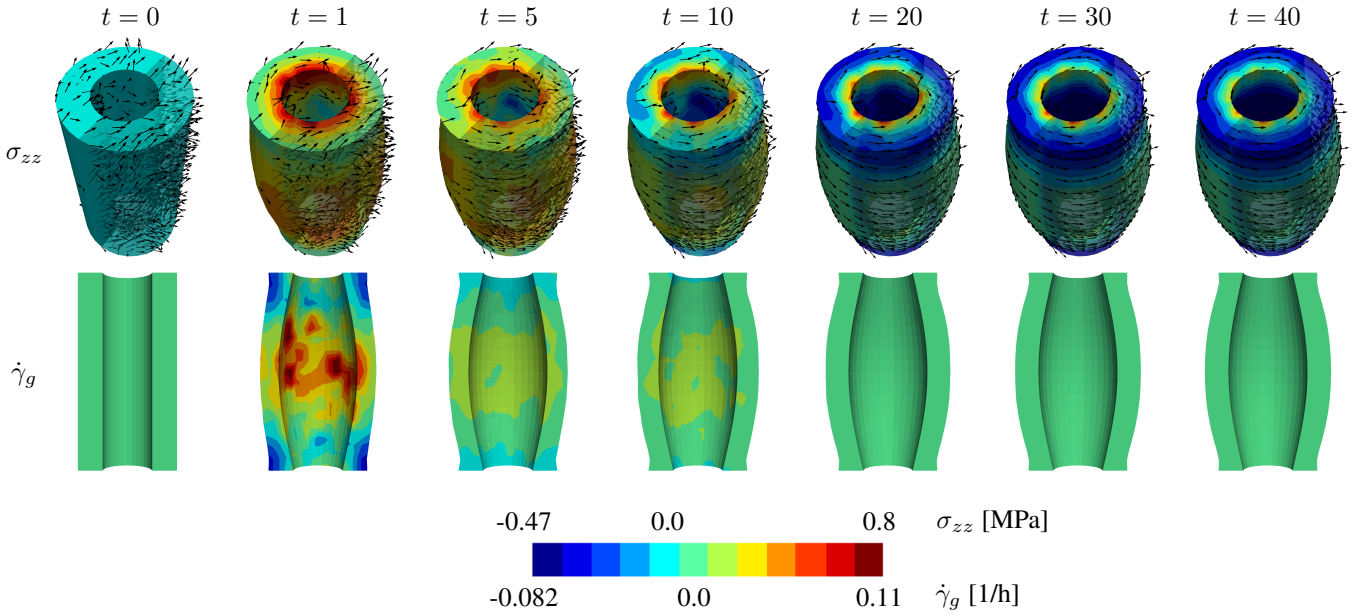

Fig. 3: Top: Cauchy stress σ_{zz} in longitudinal (z) direction at different time steps. Further, the reorientation of collagen fibers is visualized. Bottom: Growth multiplier $\dot{\gamma}$ at different time steps. A zero value corresponds to a stress state lying on the homeostatic surface.

5 Conclusion and outlook

This work has addressed both a novel co-rotated formulation of the intermediate configuration and a stress-driven growth model based on this formulation. The former is extremely advantageous when it comes to the application of AD tools for the implementation of material models based on the multiplicative decomposition of the deformation gradient.

The soft tissue material model derived from the latter takes into account both reorientation of collagen fibers and homeostasis. The latter is described by homeostatic surfaces. These surfaces are similar to yield criteria in plasticity, i.e. they describe a surface in the principal stress state. Contrary to plasticity, growth and remodeling always takes place until the current stress state lies on this surface. Here, a surface in terms of the overall Cauchy stress was chosen for this purpose.

Collagen fibers are assumed to align with the principal eigenvector of the Cauchy stress tensor. To avoid objective rates of the corresponding evolution equation, a polar decomposition of the deformation gradient was used.

Finally, the material model was examined on the basis of a structural example. It was shown that both the state of homeostasis and an orientation of the fibers in the main tensile direction can be simulated. Future work should focus on the determination of the homeostatic area, as well as the comparison with experiments.

Acknowledgements The authors gratefully acknowledge financial support of the projects RE 1057/44 (project number 465213526) and RE 1057/45 (project number 403471716) by the German Science Foundation (DFG). Further, T. Brepols and S. Reese thankfully acknowledge the funding of the project RE 1057/51 (DFG, project number 453715964). L. Lamm and S. Reese acknowledge the funding of the project 21348 N/3 by the Industrielle Gemeinschaftsforschung (IGF). Open access funding enabled and organized by Projekt DEAL.

References

[1] H. Holthusen, T. Brepols, S. Reese, and J.-W. Simon, Jour. Mech. and Phy. Sol. **163**, 104833 (2022).
[2] M. Soleimani, N. Muthyala, M. Marino, and P. Wriggers. Jour. Mech. and Phy. Sol **144**, 104097 (2020).
[3] J. F. Eichinger, L. J. Haeusel, D. Paukner, R. C. Aydin, J. D. Humphrey, and C. J. Cyron, Bio. Mod. Mech. **20**, 833–850 (2021).
[4] L. Lamm, H. Holthusen, T. Brepols, and S. Reese, Bio. Mod. Mech. **21**, 627-645 (2022).
[5] E. Rodriguez, A. Hoger, and A. McCulloch, Journal of Biomechanics **27**, 455-467 (1994).
[6] S. Reese, Int. Jour. Sol. and Struct. **40**, 951-980 (2003).
[7] W. Dettmer, and S. Reese, Comp. Meth. in Appl. Mech. and Eng. **193**, 87-116 (2004).
[8] B. Svendsen, Int. Jour. Sol. and Struct. **38**, 9579-9599 (2001).
[9] P. Perzyna, Advances in Applied Mechanics **9**, 243-377 (1966).
[10] A. Menzel, Bio. Mod. Mech. **3**, 147-171 (2005).
[11] G. A. Holzapfel, T. C. Gasse, and R. W. Ogden, Jour. Elas. and Phys. Scie. Sol. **61**, 1-41 (2000).
[12] G. Himpel, A. Menzel, E. Kuhl, and P. Steinmann, Int. Jour. Num. Meth. in Eng. **73**, 1413-1433 (2008).
[13] O. Barfusz, T. Brepols, T. van der velden, J. Frischkorn, and S. Reese, Comput. Methods Appl. Mech. Engrg. **373**, 113440 (2021).